Electrical and Mechanical Properties of Carbon-Black-Filled, Electrospun Nanocomposite Fiber Webs

Jeesang Hwang,[1] John Muth,[2] Tushar Ghosh[1]

[1]Fiber and Polymer Science Program, North Carolina State University, Raleigh, North Carolina 27695
[2]Department of Electrical and Computer Engineering, North Carolina State University, Raleigh, North Carolina 27695

ABSTRACT: The development of flexible and compliant conductive polymer composites with textile-like characteristics remains an important endeavor in light of the recent activity in polymer/textile-based electronics and the need for compliant electrodes for electroactive polymer actuators. In this work, carbon black (CB) was dispersed in a polymer solution to form electrospun fiber webs consisting mainly of nanofibers. The effect of the filler content on the fiber-web morphology, mechanical behavior, electrical conductivity, and thermal resistance was examined. The electrical conductivity percolation threshold of the fiber-web structure was found to be around 4.6 vol %. Scanning electron micrographs of the fiber webs revealed a significant influence of the CB content on the fiber formation as well as the bond structure of the fiber web, which influenced the mechanical properties of the web. © 2007 Wiley Periodicals, Inc. J Appl Polym Sci 104: 2410–2417, 2007

Key words: additives; elastomers; fibers; nanocomposites; polyurethanes

INTRODUCTION

In comparison with single-phase materials, the use of composite materials allows additional degrees of design freedom with which the physical properties of composites can be tailored for specific applications. Electrically conductive polymer matrix composites have attracted a great deal of interest because of their unique multifunctional properties, such as the ability to combine flexibility with conductivity. Compared with metals, they also are lighter in weight and can potentially be easier to process. Specifically, normally insulating polymers with good mechanical properties, such as polyurethane (PU) and polyethylene, can be made conductive by the addition of nano-sized-to-microsized conductive fillers such as graphitic particles, carbon black (CB), carbon nanotubes (CNTs), or metallic particles such as colloidal silver or gold. Carbonaceous fillers have been routinely added to many polymers for various physical property enhancements, including improvements to the electrical conductivity for electrostatic discharge protection and electromagnetic interference shielding and improvements to the thermal resistance or mechanical properties such as the yield strength.[1–4]

Conductive polymer composites are typically investigated in film form to elucidate their bulk behavior. However, polymers in thin-film form can have limited flexibility or can be fragile mechanically. To improve the mechanical characteristics while maintaining desired electrical conductivity, the use of fiber webs can be desirable because the fiber structure can provide flexibility to otherwise stiff materials, and the fiber network can provide structural strength.

Conductive fibers can be produced with a number of techniques. These include the spinning of intrinsically conductive polymers[5] and incorporating conducting fillers into an insulating polymer matrix to form fibers.[6,7] The spinning of intrinsically conducting polymers, however, presents many problems, including the low solubility of the polymer. The relatively low conductivity of conductive polymers can also be limiting. On the other hand, a significant increase in the fiber conductivity can be achieved by the incorporation of conductive particles into the fiber-forming polymer while suitable properties are maintained for spinning. Among the available fillers, CB and CNTs have been used extensively because of their ability to impart high electrical conductivity to a polymer matrix at a relatively low filler content.[1,2,6,7] CB has been used widely in conventional polymer composites because of the relative advantages of low cost, small particle size (high surface area), and aggregation behavior. CB-filled polymer composites in film form have been investigated for various applications, including sensors,[8] electrodes,[9]

and electromagnetic interference shielding.[10] However, the investigation of CB/polymer composite behavior in fiber-web form has been very limited. CB-filled electrospun fiber webs of various polymers have been investigated to thermally induce color changes in electrospun webs.[11] The fiber morphology (e.g., fineness and length) and fiber-web structural features such as the bond density, as well as other fiber characteristics determined by interactions between the polymer matrix and CB particles, have also been found to influence the mechanical properties of nanocomposite fiber webs.[12–14]

Electrospinning provides a convenient route to fabricate fiber webs of nanofibers. It is a simple process for forming nanoscale-to-microscale fibers with diameters ranging from tens of nanometers to micrometers. Numerous experimental and theoretical studies have been published to elucidate factors, such as the solution viscosity, solution conductivity, surface tension, and electric field intensity, that markedly influence the morphology of the resulting (nano)fibers and the process itself.[15,16] Because of the outstanding advantages of nanoscale fibers and relative ease of spinning a variety of polymers, electrospun fiber webs have been evaluated for many applications, including tissue engineering,[17] filtration,[18] sensors,[19] superhydrophobic surfaces,[20] electrodes in supercapacitors,[21] and composite fibers.[6,7,22]

PU has been electrospun by many, primarily to combine its intrinsic properties, such as high elasticity and flexibility, with the advantages of nanofibers.[13,15,23–25] The morphology and mechanical behavior of electrospun PU fiber webs have been investigated in terms of the fiber-bonding structure[23,24] and strain-induced molecular orientation.[25] PU has also been electrospun with various fillers to prepare nanocomposite fiber webs with enhanced mechanical properties.[13,26] Although we have focused exclusively on PU–CB composites, the electrical and other properties of other polymer systems have also been improved by the addition of CB.[1,2]

Percolation theory has been used extensively to investigate composites formed from conducting particles dispersed in an insulating host medium. As the amount of the conducting filler material increases, the composite undergoes an insulator-to-conductor transition when a conducting path is established between two boundaries.[1,2] A crucial aspect of the fabrication of conductive polymer composites is to understand the minimum amount of the conductive filler material for which this conduction occurs, which is called the *percolation threshold*. In general, the percolation threshold should be as low as possible and still allow the composite to fulfill its electrical requirements. In the literature, several processing techniques have been introduced to lower the three-dimensional percolation threshold. These include multiple percolation (especially double percolation), accumulation of a conductive filler at the continuous interfaces of multicomponent blends, and *in situ* polymerization of the polymer matrix in the presence of conductive fillers.[27,28] However, the percolation behavior of a deformable fibrous network has not been examined.

This work was motivated by the lack of reported studies of polymer composites in fiber-web form. Fiber-based composites of PU, which can potentially be used as compliant electrodes or sensors, were prepared with electrospinning. Their mechanical properties, morphological features, and electrical properties were investigated as functions of the filler concentration.

EXPERIMENTAL

Materials

The thermoplastic PU elastomer (Pellethane 2103-70A) used in this study is a commercially available polymer manufactured by Dow Chemical Co. (Midland, MI). The conductive filler CB (Ketjenblack EC-300 J) is manufactured by Akzo Nobel (Chicago, IL). CBs are characterized by their structure: a high-structure CB consists of many primary nanoparticles fused together in a grapelike aggregate. Ketjenblack EC is a high-structure CB composed of prime particles fused into primary aggregates. The diameter of the primary carbon particles used in this research was about 30 nm.[29]

Specimen preparation: Compounding and electrospinning

The composite fiber web studied in this research was produced by electrospinning.[15,16] In the electrospinning process, an electric field is used to draw a charged polymer solution or melt from an orifice (usually a syringe tip) to a collector, often a metal plate or screen. As the electric filed is increased, the hemispherical form of the solution or melt droplet held at the end of the orifice is elongated to form a conical shape, which is called a Taylor cone. The electric field is increased until it exceeds the surface tension of the first solution drop, exiting the orifice of the spinneret. The electrostatic forces transform the Taylor cone into a continuous jet of polymer from the orifice to the grounded collection surface. The discharged polymer jet undergoes a whipping process as the solvent evaporates, forming solid fibers. The fibers are collected on the grounded collection surface in the form of a fiber web.

The dispersion of CB and the dissolution of the PU–CB composite system for electrospinning were performed in a mixture of *N,N*-dimethylformamide

(DMF) and chloroform (50/50 v/v) at room temperature. First, a stable CB suspension was obtained by a CB/DMF/chloroform suspension being held for 1.5 h in an ultrasonic bath (1510-MTH, Bransonic, Bronson Ultrasound Corp., Danbury, CT). Then, PU was dissolved in a stable suspension of CB in DMF/chloroform (50/50 v/v) at room temperature. The PU–CB overall weight concentration was fixed around 12.25 wt % to ensure steady electrospinning conditions. The concentration of CB was varied between 0 and 9.46 vol % (nominal) to obtain various CB volume concentrations in the composite fiber webs, whereas the PU concentrations was altered to keep the overall concentration fixed. Solutions containing higher levels of CB were impossible to spin because of the high viscosity and discontinuity in the flow.

In the electrospinning process, the polymer solution was placed in a syringe with a needle with an inner diameter of 0.21 mm. Randomly oriented nanofibers were electrospun by the application of a voltage of ~ 25 kV to the needle with a high voltage supplier (ES30N, Gamma, Gamma High Voltage Research, Ormond Beach, FL). The grounded drum collector was located at a distance of 20 cm, and the polymer solution was fed at a rate of 80 µL/min by a syringe pump (Genie, Kent Scientific Corp., Torrington, CT). All electrospun composite fiber webs produced were dried *in vacuo* for 1 week to ensure the complete evaporation of the solvents.

Solution topography

The critical properties of particle-filled polymer composites are influenced by three primary characteristics of the filler: the particle size, polymer-to-filler interaction, and uniformity of the particle dispersion.[1] The optimal dispersion is achieved when the CB particles are separated into discrete primary aggregates. During the dispersion–fabrication step, the breakdown of aggregates and agglomeration–deagglomeration processes occur, affecting the performance and reproducibility of the composite. High-structure blacks are especially prone to breakdown. To assess the level of dispersion, the solutions prepared for electrospinning were evaluated in terms of the dispersed particle size with an Olympus BX 60 optical microscope (Olympus America, Center Valley, PA) with PAX-it-M1243 Modulator 20X software. Figure 1 shows the topography of a CB-filled [7.47 vol % (nominal)] solution before electrospinning. It shows that the CB particles were well dispersed in the solution. Limited analysis of the optical images showed an aggregate size in the range of 400–1700 nm, indicating the efficacy of ultrasonication as a means of dispersing CB particles.
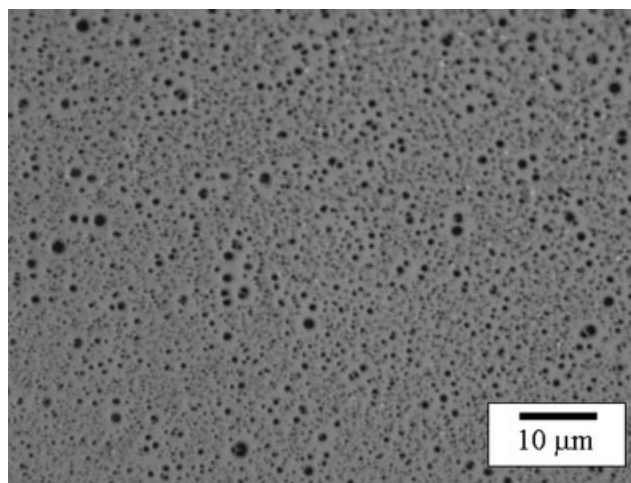
Figure 1 Optical micrograph of a CB-filled [7.47 vol % (nominal)] PU solution in DMF and chloroform.

Characterization

The electrical conductivity of the fiber webs was measured at the ambient temperature with the standard four-point probe technique. A Keithley 220 current source and a Keithley 6517A electrometer were used to measure the current–voltage characteristics of the samples. In four-point probe measurements, if the sample thickness (t) is less than the probe spacing, the resistivity (ρ) can be calculated with the following relationship:[30]

$$\rho = 4.532t\frac{V}{I} \qquad (1)$$

where V is the potential across the voltage probes and I is the current. The average ρ value of each specimen was obtained from 30 repeated measurements at various positions of the sample. The fiber-web conductivity (σ), presented later, was simply the reciprocal of ρ: $\sigma = 1/\rho$.

The morphology of the composite fiber webs was examined with a Hitachi S-3200 (Hitachi Hi-Tech Science Systems Corp., Ibarki, Japan) high-resolution scanning electron microscope. The fiber mean diameter was measured from these images with image analysis software (Image J, version 1.34 s). The measurement of the mean diameter was based on the diameters of fibers from 100 different random locations. The thermal stability of the nanofiber webs was studied by thermogravimetric analysis (TGA) with a TA Instruments (New Castle, DE) 1000 series thermal analysis system. All samples were heated from room temperature to 900°C at a scanning rate of 10°C/min in a nitrogen atmosphere. The quasi-static tensile behavior of the fiber webs was determined with an MTS (MTS System Corp., Eden Prairie, MN) 30G standard tensile load frame. To
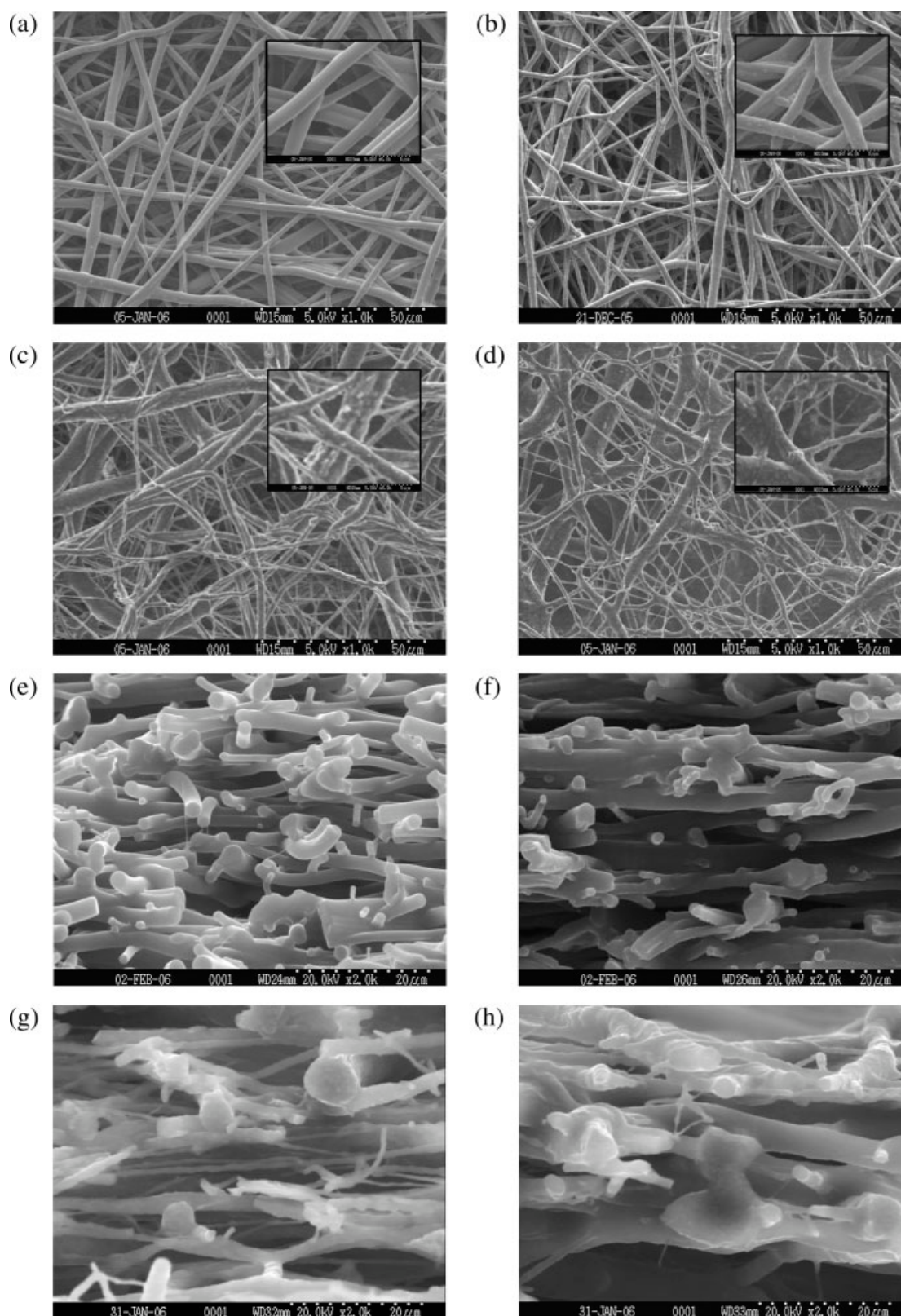
Figure 2 (a–d) Surface-scan and (e–h) cryofractured-surface scanning electron micrographs of CB–PU composite electrospun fiber webs at various CB concentrations: (a,e) 0, (b,f) 5.54, (c,g) 7.47, and (d,h) 9.46 vol %.

normalize the load data, the sample thicknesses were measured with a L&W model 51 micrometer (Lorentgen & Wettre, Sweden) at a normal pressure of 7.3 ± 0.3 psi. The reported values for the tensile modulus, strength, and elongation at break were obtained from the results of five tests.
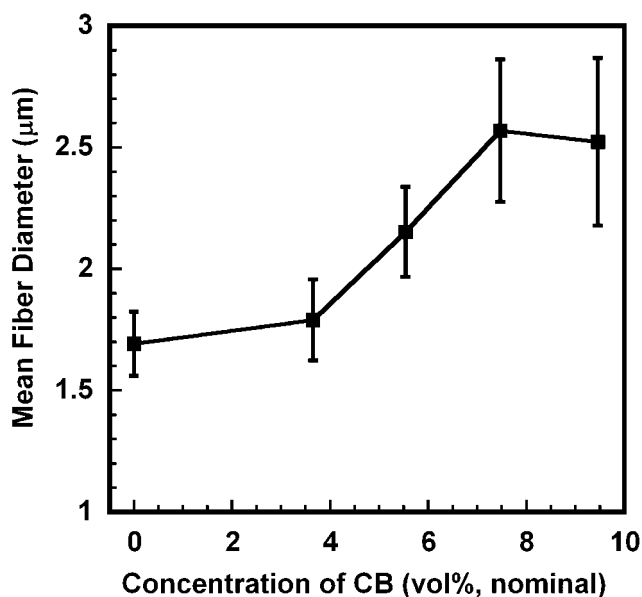
Figure 3 Variation of the mean diameter of the electrospun fibers as a function of the nominal CB content (vol %). The error bars correspond to 95% confidence intervals.

RESULTS AND DISCUSSION

Morphological characteristics and fiber diameters

A series of scanning electron micrographs of nanocomposite fiber webs with various levels of CB are presented in Figure 2. At higher levels of CB, the fiber surfaces are increasingly irregular, and the agglomeration of CB particles is apparent on the fiber surfaces, particularly near and beyond the threshold concentrations [Fig. 2(b)]. The influence of the CB content on the fiber dimensions and uniformity may not be obvious from the images in Figure 2. However, the measured values of the fiber diameter and its distribution presented as a function of the filler concentration in Figure 3 show increasing fiber diameter and greater variability in the fiber size distribution for higher CB contents. In addition, the images [Fig. 2(a–h)] also show higher fiber-to-fiber bond density for increased CB content. The difference is most likely due to the slow rate of solvent evaporation during the fiber formation between the spinneret and the collection surface due to the presence of more CB particles at the higher volume concentrations and their tendency to absorb[31] and thereby slow down the evaporation of solvents. The Ketjenblack used in this study is composed of very porous carbon particles with a dibutylphtolate (DBP) value (i.e., the volume ratio of DBP to oil that can be absorbed by 100 g of CB particles) of about 350 cm³/ 100 g.[29] This CB structure is more likely to absorb and slow down the evaporation of solvents. For the same reason, higher resolution images of the fractured nanocomposite fiber webs show evidence of

irregular and sometimes indistinct fiber formation in the fiber web [see Fig. 2(g,h)]. These observations are of interest because a higher bond density is likely to improve electron transport through the fiber web.

Mechanical properties of the composite fiber webs

The close observation of typical stress–strain curves of various PU–CB nanocomposite fiber webs presented in Figure 4 reveals some interesting features. The initial modulus of the composite fiber web increases gradually with an increase in the CB content, increasing from 0.74 MPa for 0% CB to 1.1 MPa for 7.47% CB. Subsequently, the initial modulus increases about fivefold to 3.75 MPa with 9.46 vol % (nominal) filler. In the case of the tensile strength, the data presented in Table I suggests a significant improvement at low loadings of up to 3.65% CB; however, at higher concentrations, the strength drops below that of the pristine polymer. The extension at failure was found to be highly sensitive to the addition of fillers and drops significantly with 1.80% CB. At higher levels of CB, the values seem to be fluctuating but staying at a low level compared with the elongation at break of fiber webs with no filler. The overall stress–strain behavior of fiber-web structures in this study is largely consistent with what has been reported for thermally point-bonded nonwovens.[32,33] The increases in the bond density and the overall area of the bonds for higher CB contents as well as the reinforcement effect of high-modulus CB particles are likely to improve the modulus of the fiber web. On the other hand, the diminishing strain at failure is most likely caused by the reduced degrees of freedom
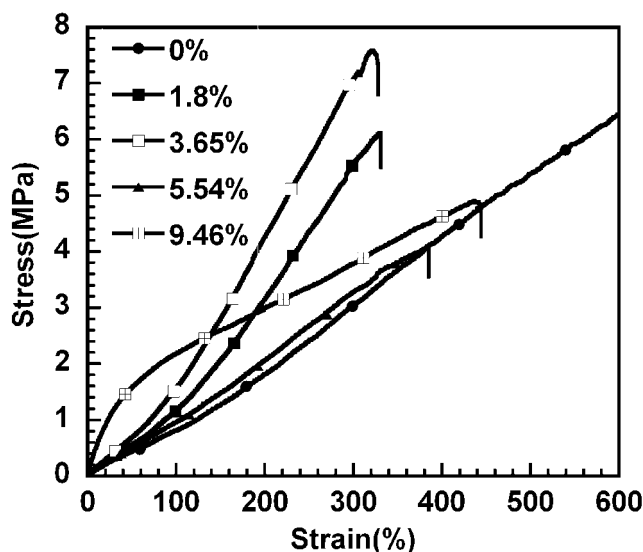
Figure 4 Typical stress–strain curves of the CB–PU electrospun fiber webs with various filler contents (all CB contents are nominal volume percentages).

TABLE I
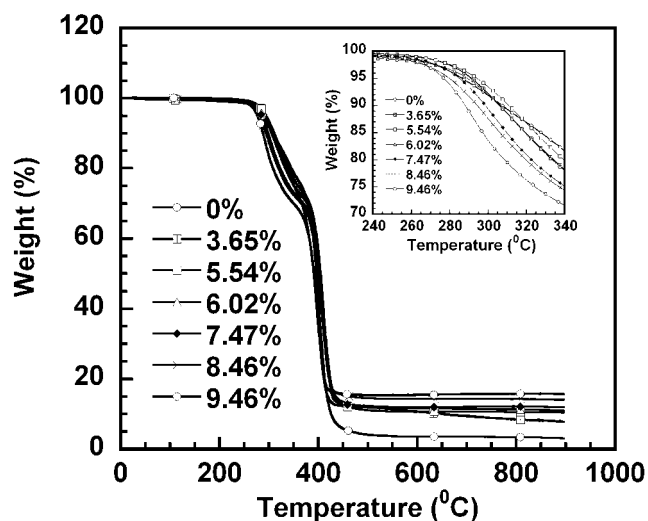**Tensile Behavior of CB–PU Composite Electrospun Fiber Webs**

Nominal CB content (vol %)	Initial modulus (MPa)	Tensile strength (MPa)	Elongation at break (%)
0.00	0.74 ± 0.16	6.06 ± 1.26	613.51 ± 32.06
1.80	1.03 ± 0.06	6.2 ± 0.96	332.92 ± 35.51
3.65	1.05 ± 0.27	7.48 ± 1.02	322.22 ± 14.51
5.54	1.08 ± 0.10	3.32 ± 0.44	349.51 ± 38.60
7.47	1.10 ± 0.04	3.06 ± 0.24	400.63 ± 15.19
8.46	2.04 ± 0.27	3.82 ± 0.41	350.82 ± 26.45
9.46	3.75 ± 0.86	4.74 ± 0.87	473.51 ± 34.15

The 95% confidence intervals are shown with the data.

of the fibers due to higher bonding as well as the stiffening of the fibers due to reinforcement. In other studies of electrospun webs, Benli et al.[34] reported a twofold increase in the initial modulus with 12 wt % CB in composite films of PU. The addition of CB to various other polymers also generally increased the modulus of the composites.[34,35] The tensile strength and initial modulus values obtained in this study compare very well with the data reported by Lee et al.[23] for electrospun Pellethane 2363-80AE, which is similar in its chemical structure to the Pellethane 2103-70A used in this research.

Thermal analysis

To ascertain the CB content and investigate the effects of CB on the thermal stability of the composite fiber web, TGA was performed on all composite samples. The changes in the weights of various CB/PU fiber webs as a function of temperature are plotted in Figure 5. A close examination of the TGA data presented in Figure 5 and Table II shows improved thermal stability of the composite fiber web with relatively low CB contents up to 5.54 vol % (nominal). The decomposition temperature is noted at 284°C with 5.54 vol % (nominal) CB versus 276°C for the pristine polymer fiber web. However, with a subsequent increase in the CB content to 7.47 vol % (nominal) and higher, the decomposition temperature is reduced to 276°C and lower. The thermal stability is generally expected to improve with the incorporation of more thermally stable fillers such as CNT and CF into fibers;[36,37] additionally, as argued by Shaffer and Windle[38] for CNT composites, the adsorption of free radicals by the CNT surface helps to improve it. This could possibly be due to the agglomeration of CB at higher loadings. Similar results have been reported in the literature for CNT–polymer composites[38,39] and organo-clay–polymer composites.[40]

The mass loss due to CB oxidation was minimized by the nitrogen environment in which the TGA was carried out, whereas the PU matrix thermally decomposed almost completely after being heated to 900°C. The mass remaining was almost entirely due to the CB, and the actual CB content of various fiber webs was computed from the residues. The results are also summarized in Table II. Actual

Figure 5 TGA of CB–PU electrospun fiber webs in a nitrogen atmosphere. The inset shows the onset of decomposition in detail (all CB contents are nominal volume percentages).

TABLE II
Decomposition Temperatures of Various CB–PU Composite Electrospun Fiber Webs and Actual CB Contents Determined from TGA

CB content				
Nominal		Measured		Decomposition temperature (°C)[a]
wt %	vol %	wt %	vol %	
0.00	0.00	0.00	0.00	276.40
5.88	3.65	4.66	2.87	283.18
8.82	5.54	7.35	4.58	284.35
9.56	6.02	7.87	4.92	277.90
11.76	7.47	8.90	5.58	276.60
13.23	8.46	11.02	6.98	270.50
14.71	9.46	12.60	8.03	269.70

[a] Temperature at a 3 wt % loss.
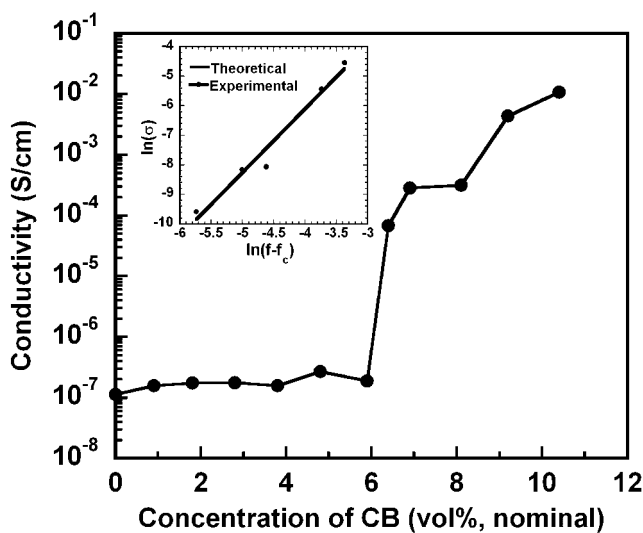
Figure 6 Electrical conductivity of the PU–CB electrospun fiber webs as a function of the filler content. The inset shows the fit of the experimental data to the power law of percolation [eq. (2)].

weight fractions of CB in the fiber webs were found to be significantly lower than their nominal values. The most likely reason is the loss of CB particles during the preparation of the CB suspension and subsequent mixing with the polymers followed by electrospinning from a syringe. Even with continuous agitation during the processing, a small amount of CB precipitated, causing a lower actual CB content in the fiber web.

Electrical conductivity and percolation behavior

The variation in the direct-current conductivity of the nanocomposite fiber webs with respect to the filler concentration is shown in Figure 6. The conductivity of the pure PU fiber web was measured at about 1.14×10^{-7} S/cm. A sharp increase in the conductivity of approximately 3 orders of magnitude was recorded between filler contents of 5.54 and 6.02 vol % (nominal). As the filler concentration increased from 5.54 to 6.02 vol % (nominal), the conductivity increased from about 1.88×10^{-7} to about 6.80×10^{-5} S/cm. After that, the conductivity changed only moderately, increasing to about 1.07×10^{-2} S/cm for 9.46 vol % (nominal) filler. This behavior is indicative of a percolation transition. As shown in Figure 6, the percolation threshold of the PU–CB nanocomposite fiber web lies between 5.54 and 6.02 vol % (nominal) CB. In light of the TGA data presented earlier, this represents an actual CB content between 4.58 and 4.92 vol %. Percolation thresholds for various CB composites, including PU–CB composites, have been reported to be in the range of 2–12 vol %.[41–43]

The electrical conductivity of a composite (σ_c) above the percolation threshold can be expressed as follows:[44]

$$\sigma_c = \sigma_0(f - f_c)^t \quad \text{for } f > f_c \tag{2}$$

where σ_0 is the constant of proportionality, f is the volume fraction of the conducting filler in the composite, f_c is the critical volume fraction (volume fraction at percolation), and t is a critical exponent. The value of t is expected to be material-independent[45] and is considered indicative of the strength of the percolation transition. For any three-dimensional system, t yields a value of about 2.0.[46] An analysis of our data presented in the inset of Figure 6 resulted in a value for t of 2.165 when the percolation threshold was assumed to be 4.6 vol % (actual). The inset of Figure 6 shows a plot of our data in the form of the power-law relation of eq. (1). The value of t is in line with what has been reported in the literature for CB-filled polymer composites and in particular for high-structure CB-filled composites.[47] The apparent tunneling–percolation behavior of the CB–PU composite in the fiber-web form remains a subject of investigation.

CONCLUSIONS

This report describes a successful and unique route for fabricating porous conducting composite fiber webs containing CBs. The results clearly demonstrate the efficacy of incorporating CB into the PU matrix with electrospinning. The influence of higher CB contents on the electrospun fibers manifested in larger fibers as well as higher bond densities. The initial modulus of the fiber web increased substantially with increasing CB content. The presence of CB increased the fiber web strength marginally up to 3.65 vol % (nominal) CB and fell significantly beyond that. The electrical conductivity, as well as thermal stability, increased significantly up to about 5.54 vol % (nominal) CB. The electrical conductivity of the composite fiber web increased about 3 orders of magnitude when the filler content increased from 5.54 to 6.02 vol % (nominal). The percolation threshold of conductivity was determined to be between 4.58 and 4.92 vol % (actual) CB. The critical exponent of percolation (t) was calculated to be 2.165 when the percolation threshold was assumed to be around 4.6 vol % (actual). The results seem to confirm the tunneling–percolation behavior of the CB–PU composite fiber web investigated in this research.

References

1. Huang, J. Adv Polym Technol 2002, 21, 299.
2. Chung, D. D. L. J Mater Sci 2004, 39, 2645.
3. Thosenson, E. T.; Ren, Z.; Cou, T. Compos Sci Technol 2001, 61, 1899.

4. Calvert, P. Nature 1999, 399, 210.
5. Kang, T. S.; Lee, S. W.; Joo, J.; Lee, J. Y. Synth Met 2005, 153, 61.
6. Munoz, E.; Suh, D.; Collins, S.; Selvidge, M.; Dalton, A. B.; Kim, B. G.; Razal, J. M.; Ussery, G.; Rinzler, A. G.; Martinez, M. T.; Baughman, R. H. Adv Mater 2005, 17, 1064.
7. Seoul, C.; Kim, Y.; Baek, C. J Polym Sci Part B: Polym Phys 2003, 41, 1572.
8. Chen, S. G.; Hu, J. W.; Zhang, M. Q.; Rong, M. Z.; Zheng, Q. Sens Actuators B 2006, 113, 361.
9. Richner, R.; Muller, S.; Wokaun, A. Carbon 2002, 40, 307.
10. Bigg, D. M.; Stutz, D. Polym Compos 1983, 4, 40.
11. Pedicini, A.; Farris, R. J. J Polym Sci Part B: Polym Phys 2004, 42, 752.
12. Inai, R.; Kotaki, M.; Ramakrishna, S. J Polym Sci Part B: Polym Phys 2005, 43, 3205.
13. Hong, J. H.; Jeong, E. H.; Lee, H. S.; Baik, D. H.; Seo, S. W.; Youk, J. H. J Polym Sci Part B: Polym Phys 2005, 43, 3171.
14. Choi, S. S.; Lee, S. G.; Joo, C. W.; Im, S. S.; Kim, S. H. J Mater Sci 2004, 39, 1511.
15. Theron, S. A.; Zussman, E.; Yarin, A. L. Polymer 2004, 45, 2017.
16. Fridrikh, S. V.; Yu, J. H.; Brenner, M. P.; Rutledge, G. C. Phys Rev Lett 2003, 90, 144502.
17. Xu, C. Y.; Inai, R.; Kotaki, M.; Ramakrishna, S. Biomaterials 2004, 25, 877.
18. Tsai, P. P.; Schreuder-Gibson, H.; Gibson, P. J Electrostatics 2002, 54, 333.
19. Kessick, R.; Tepper, G. Sens Actuators B 2006, 117, 205.
20. Ma, M.; Mao, Y.; Gupta, M.; Gleason, K. K.; Rutledge, G. C. Macromolecules 2005, 38, 9742.
21. Kim, C.; Yang, K. S. Appl Phys Lett 2003, 83, 1216.
22. Ge, J. J.; Hou, H.; Li, Q.; Graham, M. J.; Greiner, A.; Reneker, D. H.; Harris, F. W.; Cheng, S. Z. D. J Am Chem Soc 2004, 126, 15754.
23. Lee, K. H.; Kim, H. Y.; Ryu, Y. J.; Kim, K. W.; Choi, S. W. J Polym Sci Part B: Polym Phys 2003, 41, 1256.
24. Kidoaki, S.; Kwon, I. K.; Matsuda, T. J Biomed Mater Res Part B 2006, 76, 219.
25. Pedicini, A.; Farris, R. J. Polymer 2003, 44, 6857.
26. Sen, R.; Zhao, B.; Perea, D.; Itkis, M. E.; Hu, H.; Love, J.; Bekyarova, E.; Haddon, R. C. Nano Lett 2004, 4, 459.
27. Gubbels, F.; Jerome, R.; Teyssie, P.; Vanlathem, E.; Deltour, R.; Calderone, A.; Parente, V.; Bredas, J. L. Macromolecules 1994, 27, 1972.
28. Thongruang, W.; Spontak, R.; Balik, C. M. Polymer 2002, 43, 3717.
29. Mallette, J. G.; Quej, L.; Marquez, A.; Manero, O. J Appl Polym Sci 2001, 81, 562.
30. Wiegenstein, C.; Schulza, K. Rev Sci Instrum 1997, 68, 1812.
31. Lawandy, S. N.; Wassef, M. J Appl Polym Sci 1990, 40, 323.
32. Michielsen, S.; Pourdeyhimi, B.; Desai, P. J Appl Polym Sci 2006, 99, 2489.
33. Batra, S. K.; Davis, H.; Dharmadhikary, R. K.; Gilmore, T. F. Text Res J 1999, 69, 725.
34. Benli, S.; Yilmazer, U.; Pekel, F.; Ozkar, S. J Appl Polym Sci 1998, 68, 1057.
35. Flandin, L.; Hiltner, A.; Baer, E. Polymer 2001, 42, 827.
36. Wang, Y.; Cheng, R.; Liang, L.; Wang, Y. Compos Sci Technol 2005, 65, 793.
37. Ma, H.; Zeng, J.; Realff, M. L.; Kumar, S.; Schiraldi, D. A. Compos Sci Technol 2003, 63, 1617.
38. Shaffer, M. S.; Windle, A. Adv Mater 1999, 11, 937.
39. Velasco-Santos, C.; Martinez-Hernandez, A. L.; Fisher, F.; Ruoff, R.; Castano, V. M. J Phys D: Appl Phys 2003, 36, 1423.
40. Chang, J. H.; Park, D. J Polym Sci Part B: Polym Phys 2001, 39, 2581.
41. Xiong, C.; Zhou, Z.; Xu, W.; Hu, H.; Zhang, Y.; Dong, L. Carbon 2005, 43, 1778.
42. Heiser, J. A.; King, J.; Konell, J. P.; Sutter, L. L. Adv Polym Technol 2004, 23, 135.
43. Flandin, L.; Chang, A.; Nazarenko, S.; Hiltner, A.; Baer, E. J Appl Polym Sci 2000, 76, 894.
44. Kirkpatrick, S. Rev Mod Phys 1973, 45, 574.
45. Stauffer, D.; Aharony, A. Introduction to Percolation Theory; Taylor & Francis: London, 1994.
46. Batrouni, G. G.; Hansen, A.; Larson, B. Phys Rev E 1996, 53, 2292.
47. Balberg, I. Carbon 2002, 40, 139.